Photochemistry and Photobiology, 1996, 63(6): 735–741

Symposium-in-Print

Detailed Mechanism of Phenol-Inhibited Peroxidase-Catalyzed Oxidation of Indole-3-Acetic Acid at Neutral pH*

Sergey N. Krylov and H. Brian Dunford†

Department of Chemistry, University of Alberta, Edmonton, Alberta, Canada

Received 12 October 1995; accepted 9 January 1996

ABSTRACT

The inhibition of horseradish peroxidase (HRP)-catalyzed oxidation of indole-3-acetic acid (IAA) by a phenol, caffeic acid (CA), was studied using both a kinetic approach and computer simulation. The presence of CA resulted in a lag period in IAA oxidation. The lag period increased slowly with increasing [CA] until a critical concentration, $[CA]_{cr}$, was reached, then it increased much faster when [CA] was greater than $[CA]_{cr}$. The $[CA]_{cr}$ was proportional to [IAA] and did not depend upon [HRP]. Caffeic acid was oxidized by compound I and compound II of HRP with bimolecular rate constants (6.8 ± 10^7 and 2.1 ± 10^7 $M^{-1}s^{-1}$), which were much higher than the corresponding rate constants for IAA oxidation (2.3 ± 10^3 and 2.0 ± 10^2 $M^{-1}s^{-1}$). Our experimental data show that CA inhibits IAA oxidation because it is able to compete effectively as a peroxidase substrate. A model based on a detailed mechanism of IAA oxidation was investigated using computer simulation. A rate constant driving nonenzymatic hydroperoxide formation in IAA solution was determined, 3.0×10^{-7} s^{-1}. The model quantitatively describes the experimental results of this work and also qualitatively explains data published earlier. The critical inhibitor concentration is approximately equal to twice the concentration of hydroperoxide in IAA solution at the time of inhibitor addition. Therefore hydroperoxide concentration can be calculated from the determination of critical inhibitor concentration.

INTRODUCTION

Indole-3-acetic acid (IAA)‡ is a natural phytohormone with many growth regulatory functions. The level of IAA in plants is, in particular, controlled *via* its enzymatic oxidation that is catalyzed by peroxidases (1). Peroxidase-catalyzed aerobic oxidation of IAA produces an electronically excited species. The chemiluminescence of these species and their chemical reactivity have been thoroughly studied by G. Cilento and co-workers for many years. They suggested a hypothesis to explain "photobiochemistry without light," discussed in detail in a number of reviews (2–5). According to this hypothesis the energy of an enzyme-generated electronically excited species can give rise to photochemical-like reactions in living systems in the dark. The intriguing results of Cilento's group stimulated a study of different aspects of IAA oxidation in our groups (in Russia and in Canada). One of us (H.B.D.) collaborated with G. Cilento for many years. Although progress in understanding the mechanisms of peroxidase-catalyzed IAA oxidation and related processes have been achieved, many questions remain unresolved.

The IAA/horseradish peroxidase (HRP)/O_2 system emits in three spectral regions: 420, 465 and 535 nm with different behavior exhibited in each region (6–8). Therefore at least three different electronically excited products (intermediates) are formed (6). Identification of these products is a complex but solvable problem. The yields of these products are very sensitive to experimental conditions, in particular, pH. At neutral pH, and under steady-state conditions of IAA oxidation, only the product emitting at 420 nm is formed (6). De Mello *et al.* (8) suggested that hydroperoxide, ROOH, which is an intermediate of IAA oxidation, is responsible for this emission. There is indirect evidence for this hypothesis. Oxidation of IAA at neutral pH goes through a peroxidase pathway accompanied by a free radical chain reaction (9,10). Our computer simulation showed that ROOH is the intermediate of highest concentration, and it reaches its steady-state concentration much later than the other intermediates (10 min and 1 min, respectively) (11). Preliminary results show that the intensity of the 420 nm chemiluminescence from the IAA/HRP/O_2 system also reaches the steady state after a long lag period (6,12). However, in order to prove a direct connection between ROOH concentration and chemiluminescence at 420 nm, the time dependence of ROOH has to be measured experimentally. A simple indirect way of ROOH measurement in the IAA/HRP/O_2 system was suggested by Nakajima and Yamazaki (9). They used ascorbate to induce a lag period in IAA oxidation. They proposed that the critical concentration of ascorbate causing a sudden in-

*This paper is dedicated to the memory of Giuseppe Cilento.

†To whom correspondence should be addressed at: Department of Chemistry, University of Alberta, Edmonton, Alberta T6G 2G2, Canada. Fax: 403-492-8231; e-mail: brian.dunford@ualberta.ca.

‡*Abbreviations:* CA, caffeic acid; HRP, HRP-I and HRP-II, native form, compound I and compound II of horseradish peroxidase, respectively; IAA and RH, indole-3-acetic acid.

crease in the lag time was equal to the concentration of ROOH. However the mechanism of the effect of ascorbate on IAA oxidation is not completely clear. Ascorbate is known to be an effective free radical scavenger (13) and at the same time a substrate for HRP-I and HRP-II. Therefore ascorbate could inhibit IAA oxidation either by free radical scavenging or by acting as a competitive substrate. In the first case there is no direct connection between ascorbate and hydroperoxide concentrations. In the second, the connection between critical concentration of ascorbate and the concentration of ROOH has to be determined. There is another reason to study the mechanism of inhibition of IAA oxidation. It is known that peroxidase-catalyzed oxidation of IAA is inhibited by naturally occurring phenols such as: caffeic, gallic, ferulic and chlorogenic acids. These phenolic compounds exhibit the same critical behavior with respect to IAA oxidation as ascorbate (14–16). The influence of the inhibitors was investigated by a number of authors (14–24). Two hypotheses where suggested to explain the inhibition: (1) the inhibitor is a competitive substrate for enzyme (19–23) and (2) the inhibitor is a scavenger of free radicals (14–18). It was difficult to prove either of these hypotheses because the mechanism of peroxidase-catalyzed IAA oxidation itself was unclear.

In our recent work we have proven that IAA oxidation at neutral pH goes through the peroxidase pathway accompanied by a free radical chain reaction (10). Moreover, a detailed model of IAA oxidation has been developed and investigated (11). Unavailable rate constants were determined either experimentally or by computation (analytical and computer) (10,11). The suggested model quantitatively describes all the available experimental results and can serve to establish new experimental and theoretical research on the processes related to IAA oxidation such as the inhibition and activation of IAA oxidation by phenolic compounds.

In this paper we report the results of a study of the inhibition of IAA oxidation by caffeic acid (CA) both kinetically and by computer simulation. Both the competitive inhibitor and free radical scavenger hypotheses are examined using a detailed model of IAA oxidation in the presence of CA. It is shown that CA acts predominantly as a competitive substrate. A critical CA concentration was found to be approximately equal to twice the hydroperoxide concentration and can be used for determination of the time dependence of [ROOH] in the IAA/HRP/O_2 system.

MATERIALS AND METHODS

Materials. The HRP (RZ = 3.0), IAA and CA were obtained from Sigma (St. Louis, MO), while the components of the phosphate and carbonate–bicarbonate buffers were purchased from Fisher Scientific (Fair Lawn, NJ).

The IAA was dissolved in hot deionized water. The HRP concentration was determined spectrophotometrically using the extinction coefficient at 403 nm of $1.02 \times 10^5\ M^{-1}\ cm^{-1}$ (25). Except where otherwise stated, the solutions were prepared in 0.1 *M* pH 7.4 phosphate buffer using deionized water. The temperature was kept at 20.0 ± 0.5°C. Prior to reaction initiation the solution of IAA was saturated with air; the initial oxygen concentration was about 0.25 m*M* at 20.0°C (26).

Methods. The kinetics of phenol-inhibited IAA oxidation and HRP-II formation during IAA oxidation were measured using a Beckman DU 650 spectrophotometer at 290 nm and 430 nm (isosbestic point between HRP and HRP-I), respectively. Kinetics were corrected for lamp intensity drift during the period of measurements. Quartz cuvettes of 1 cm pathlength were used. In all the experiments CA was first added to the IAA solution and then the reaction was initiated by the addition of enzyme; the standard reaction mixture contained 1 μ*M* HRP and 0.1 m*M* IAA in 1 mL.

Stopped-flow experiments were performed on an SX.17MV sequential stopped-flow spectrometer (Applied Photophysics, UK). The rate constant k_{12} for the reaction of HRP-I with CA was measured by following the absorbance at 411 nm (isosbestic point between HRP and HRP-II). The HRP-I was prepared by mixing equimolar amounts of HRP and H_2O_2. The HRP-I was stable for the duration of the kinetic measurements. The final HRP-I concentration was 0.3 μ*M*, while the final CA concentration was varied from 2 to 8 μ*M*.

The rate constant k_{13} for the reaction of HRP-II with CA was measured by following the absorbance at 430 nm. The HRP-II was prepared by mixing equimolar amounts of HRP, H_2O_2 and CA in 0.02 *M* carbonate–bicarbonate buffer at pH 10. The HRP-II was stable for the duration of the kinetic measurements. The final HRP-II concentration was 1 μ*M*, and the final CA concentration was varied from 10 to 35 μ*M*.

The stoichiometry of the reaction of HRP-I and ascorbate was established in an experiment in which equimolar amounts of the two reactants were mixed and the amount of HRP-II formed was measured.

Computer simulation. We used an IBM-compatible computer with a 486 coprocessor operating at 66 MHz for our computer simulation. The program for integration of reaction rate equations was designed by S.N.K. using standard Runge–Kutta routines with adaptive stepsize control (27). The program is written in FORTRAN and computes in double precision variables. The program is available upon request. The differential rate equations, the rate constants and integration parameters used in the program are listed in Tables 1 and 2.

RESULTS

Critical CA concentration

First, we studied experimentally the inhibition of IAA oxidation by CA. Increasing CA concentration resulted in increasing delay of IAA oxidation (Fig. 1). After the lag, the oxidation of IAA proceeded at the same rate as in the absence of inhibitor. The delay caused by CA was a complex function of [CA] (Fig. 2). The behavior of the system changed abruptly when a critical CA concentration ($[CA]_{cr} \approx 7 \times 10^{-8}\ M$) was reached. At [CA] < $[CA]_{cr}$, the delay in IAA oxidation increased slowly with increasing [CA] in a linear manner (Fig. 2). At [CA] > $[CA]_{cr}$, the delay as a function of [CA] also increased linearly but with considerably bigger slope. These results are in accordance with those for inhibition of IAA oxidation by ascorbate (9) and 6-chloro-4-nitro-2-aminophenol (15). The $[CA]_{cr}$ increased with increasing [IAA] and did not depend on [HRP] (Fig. 3). The results are also in good quantitative agreement with those measured by chemiluminescence (14).

Reaction model

Bimolecular rate constants of CA oxidation by HRP-I and HRP-II, k_{12} and k_{13}, were determined experimentally. The [CA] in excess of enzyme concentration was used to achieve pseudo-first-order conditions. The dependencies of k_{obs} on CA concentration were linear for both the reactions of CA with HRP-I and HRP-II (Fig. 4). The rate constants were determined from the slopes: $k_{12} = (6.8 \pm 0.2) \times 10^7\ M^{-1}\ s^{-1}$ and $k_{13} = (2.1 \pm 0.1) \times 10^{-7}\ M^{-1}\ s^{-1}$. These rate constants are five orders of magnitude higher than the rate constants of IAA oxidation by HRP-I and HRP-II (k_8 and k_9, Table 1).

Table 1. Main reactions that influence peroxidase-catalyzed oxidation of IAA in the presence of CA at pH 7.4 and their corresponding rate constants

	Reaction	Rate constants	Reference
1	$RH \rightarrow R^{\cdot}$	$k_1 = 3 \times 10^{-7}\ s^{-1}$	Present paper
2	$R^{\cdot} + O_2 \rightarrow ROO^{\cdot}$	$k_2 = 2.0 \times 10^{8}\ M^{-1} s^{-1}$	11,30
3	$ROO^{\cdot} + RH \rightarrow ROOH + R^{\cdot}$	$k_3 = 1.0 \times 10^{6}\ M^{-1} s^{-1}$	11
4	$R^{\cdot} \rightarrow P_1$	$k_4 = 1.8 \times 10^{4}\ s^{-1}$	11
5	$ROO^{\cdot} \rightarrow P_2$	$k_5 = 5.62\ s^{-1}$	11
6	$ROOH \rightarrow P_3$	$k_6 = 1.45 \times 10^{-3}\ s^{-1}$	9,11
7	$HRP + ROOH \rightarrow HRP\text{-}I + ROH$	$k_7 = 2.0 \times 10^{6}\ M^{-1} s^{-1}$	9,11
8	$HRP\text{-}I + RH \rightarrow HRP\text{-}II + R^{\cdot}$	$k_8 = 2.3 \times 10^{3}\ M^{-1} s^{-1}$	10,11
9	$HRP\text{-}II + RH \rightarrow HRP + R^{\cdot}$	$k_9 = 2.05 \times 10^{2}\ M^{-1} s^{-1}$	10,11
10	$HRP\text{-}II \rightarrow HRP$	$k_{10} = 1.75 \times 10^{-3}\ s^{-1}$	10,11
11	$HRP\text{-}I + ROOH \rightarrow P\text{-}670$	$k_{11} = 6.2 \times 10^{2}\ M^{-1} s^{-1}$	11
12	$HRP\text{-}I + CA \rightarrow HRP\text{-}II + CA^{\cdot}$	$k_{12} = 6.8 \times 10^{7}\ M^{-1} s^{-1}$	Present paper
13	$HRP\text{-}II + CA \rightarrow HRP + CA^{\cdot}$	$k_{13} = 2.1 \times 10^{7}\ M^{-1} s^{-1}$	Present paper
14	$CA^{\cdot} + CA^{\cdot} \rightarrow P_4$	—	

Therefore CA competes with IAA for oxidized enzyme species even when the concentration of CA is 10^5 times less than that of IAA. Because of this result we propose that CA inhibits IAA oxidation mainly as a competitive substrate.

The reaction scheme describing the peroxidase-catalyzed IAA oxidation in the presence of CA is shown in Fig. 5. Table 1 contains the corresponding reaction equations and rate constants. The mechanism of the phenol-inhibited IAA oxidation is based on the detailed model of the peroxidase-catalyzed IAA oxidation at neutral pH developed in our previous work (11). Reaction 1 represents a slow nonenzymatic generation of free radical R· from IAA (14,15). Reactions 2 and 3 are the free radical chain processes that regenerate free radicals R· as well as the hydroperoxide ROOH required for the initiation of the enzymatic cycle. The termination steps for R· and ROO· can be satisfactorily described by the unimolecular Reactions 4 and 5 (11). Unimolecular destruction of ROOH occurs in Reaction 6 (9). The reaction sequence 1–6 is responsible for the presence of ROOH traces in IAA solution in the absence of HRP (9,11). The IAA and CA are oxidized in the standard peroxidase cycle (Reaction 7–9, 12, 13). The HRP-II is slowly reduced in the absence of IAA and CA (Reaction 10) (10,11). For simplicity we consider this reaction to be unimolecular (11). The formation of P-670 is apparently initiated by a rate-controlling reaction of HRP-I with ROOH (9,10). Therefore we do not consider any other intermediates for P-670 formation but only Reaction 11. Finally, Reaction 14 is the recombination of CA free radicals to yield a variety of reaction products denoted as P_4. The rate constants k_2–k_{13} are known (Table 1). The rate constant k_{14} is not significant in this consideration because CA· and P_4 are products of termination reactions that do not influence the overall process. The rate constant k_1 was unknown and was fitted in the present study.

A fairly detailed model of phenol inhibition of the HRP-catalyzed IAA oxidation was proposed by Gelinas (21). The model describes a competition between inhibitor and IAA for HRP-I and HRP-II. It could not be used for computer simulation because elementary rate constants were not measured. A further disadvantage is that the model did not include a nonenzymatic chain reaction and hence critical inhibitor concentration could not be discussed.

Computer simulation

First we made an initial estimation of k_1. In previous work by Yamazaki, the steady-state concentration of hydroperoxide in 0.1 m*M* IAA solution (without HRP) was estimated to be roughly $[ROOH]_0 = 5 \times 10^{-9}\ M$ (28). We simulated the formation of ROOH in IAA solution in the absence of HRP and CA starting from [ROOH] = 0. Our calculations showed that the steady-state concentration of ROOH in IAA solution was proportional to k_1 and was reached in about 50 min; it was equal to Yamazaki's estimate when $k_1 = 6 \times 10^{-8}\ s^{-1}$.

Next we simulated IAA oxidation in the presence of HRP and CA for $k_1 = 6 \times 10^{-8}\ s^{-1}$. A delay in the initiation of IAA oxidation was observed in the simulation. Moreover, the simulated dependence of the delay on [CA] reached a critical point after which it increased abruptly, as we observed experimentally (Fig. 2). However, quantitative agreement was poor. The $[CA]_{cr}$ on the simulated curve was about one order of magnitude less than the experimentally determined $[CA]_{cr}$. An explanation is that the k_1 value was underestimated because of the previous underestimation of $[ROOH]_0$ (28). Therefore, using least-squares analysis we obtained a new value of k_1 ($3 \times 10^{-7}\ s^{-1}$), which optimized the fit of the simulated reaction to the experimental results (Fig. 2, solid line). For this value of k_1, a steady-state concentration of $[ROOH]_0 = 2.7 \times 10^{-8}\ M$ was reached in 0.1 m*M* IAA solution in the absence of HRP and CA. The simulated $[ROOH]_0$ was proportional to [IAA] and their ratio was 2.7×10^{-4}.

The next step was simulation of the influence of [IAA] and [HRP] on $[CA]_{cr}$ using the optimal value of k_1 ($3 \times 10^{-7}\ s^{-1}$). The results are shown in Fig. 3 (solid lines). It can be seen that the simulated curves satisfactorily fit the experimental results.

We also simulated addition of CA after HRP. In this case the spontaneous oxidation of IAA by HRP is started before addition of the inhibitor. Behavior of the simulated reaction was similar to that for CA addition before HRP. There was a reaction delay that increased with increasing [CA], and a $[CA]_{cr}$ beyond which the slope of the plot of delay time *vs* [CA] increased abruptly. The $[CA]_{cr}$ depended on the time

Table 2. Parameters of computer simulation

Rate equations:

$d[HRP]/dt = -k_7[HRP][ROOH] + k_9[HRP\text{-}II][RH] + k_{10}[HRP\text{-}II]$
$d[HRP\text{-}I]/dt = k_7[HRP][ROOH] - k_8[HRP\text{-}I][RH] - k_{12}[HRP\text{-}I][CA] - k_{11}[HRP\text{-}I][ROOH]$
$d[HRP\text{-}II]/dt = k_8[HRP\text{-}I][RH] - k_9[HRP\text{-}II][RH] - k_{13}[HRP\text{-}II][CA] - k_{10}[HRP\text{-}II]$
$d[P\text{-}670]/dt = k_{11}[HRP\text{-}I][ROOH]$
$d[RH]/dt = -k_8[HRP\text{-}I][RH] - k_9[HRP\text{-}II][RH] - k_3[ROO^{\cdot}][RH] - k_1[RH]$
$d[R^{\cdot}]/dt = k_8[HRP\text{-}I][RH] + k[HRP\text{-}II][RH] - k_2[O_2][R^{\cdot}] + k_3[ROO^{\cdot}][RH] - k_4[R^{\cdot}] + k_1[RH]$
$d[ROO^{\cdot}]/dt = k_2[O_2][R^{\cdot}] - k_3[ROO^{\cdot}][RH] - k_5[ROO^{\cdot}]$
$d[ROOH]/dt = -k_7[HRP][ROOH] - k_{11}[HRP\text{-}I][ROOH] + k_3[ROO^{\cdot}][RH] - k_6[ROOH]$
$d[O_2]/dt = -k_2[O_2][R^{\cdot}]$
$d[CA]/dt = -k_{12}[HRP\text{-}I][CA] - k_{13}[HRP\text{-}II][CA]$

Initial concentrations:

$[HRP]_0 = 1\ \mu M$ (except where otherwise stated)
$[RH]_0 = 0.1$ mM (except where otherwise stated)
$[O_2]_0 = 0.25$ mM
$[ROOH]_0 = 2.7 \times 10^{-4}\ [RH]_0$
All other initial concentrations except [CA] are zero.

Integration parameters:

period between HRP and CA addition to IAA (Fig. 6, curve 1). The maximum value of $[CA]_{cr}$ was obtained when CA was added 10 min after HRP. This also corresponds to the time maximum [ROOH] is observed in the simulated reaction (Fig. 6, curve 2) (11). The inset to Fig. 6 shows that the ratio $[CA]_{cr}/[ROOH]$ is close to 2 except at the very beginning and end of the reaction.

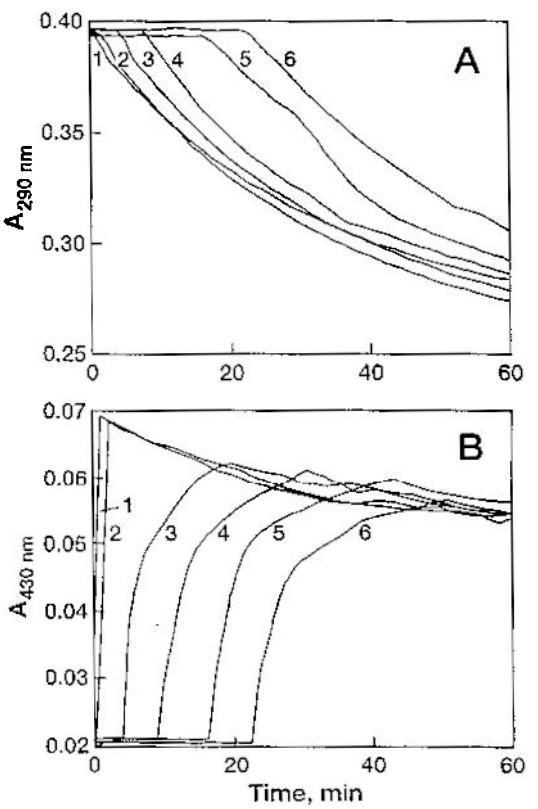

Figure 1. The effect of CA on (A) the kinetics of peroxidase-catalyzed IAA oxidation followed as an absorbance at 290 nm; (B) the kinetics of HRP-II formation during peroxidase-catalyzed IAA oxidation followed as an absorbance at 430 nm. The concentrations of CA: 0 (1), 0.04 μM (2), 0.08 μM (3), 0.12 μM (4), 0.16 μM (5), 0.20 μM (6).

DISCUSSION

Addition of CA to IAA prior to HRP addition

Traces of ROOH are always present in IAA solutions due to Reactions 1–6 (Table 1, Fig. 6). Therefore upon addition of CA and HRP to IAA the reaction mixture contains: HRP, traces of ROOH and two competing reducing substrates, IAA and CA. The HRP is oxidized by ROOH to form HRP-I. The HRP-I is then reduced to HRP-II and HRP-II is further reduced to HRP by both IAA and CA. The rate constants for the reactions of CA with HRP-I and HRP-II, k_{12} and k_{13}, are about five orders of magnitude greater than those for the reactions of IAA with HRP-I and HRP-II, k_8 and k_9. Therefore, CA effectively competes with IAA for HRP-I and HRP-II even if [CA] is much less than the [IAA].

If the concentration of added CA is less than $[CA]_{cr}$ then the steady-state $[ROOH]_0$, which was present in IAA solu-

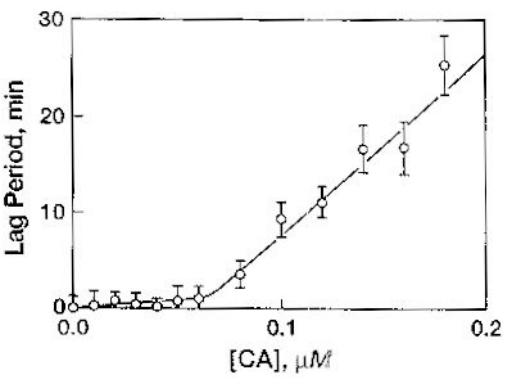

Figure 2. The delay of peroxidase-catalyzed IAA oxidation, caused by CA, as a function of [CA]. Points represent experimental data and solid line represents the results of computer simulation.

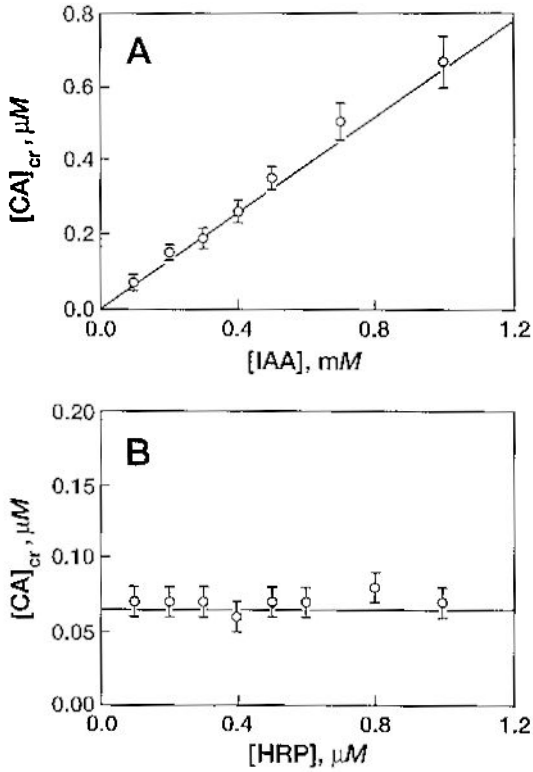

Figure 3. The effect of (A) [IAA] and (B) [HRP] on the critical [CA]. Points represent experimental data while solid lines represent the results of computer simulation.

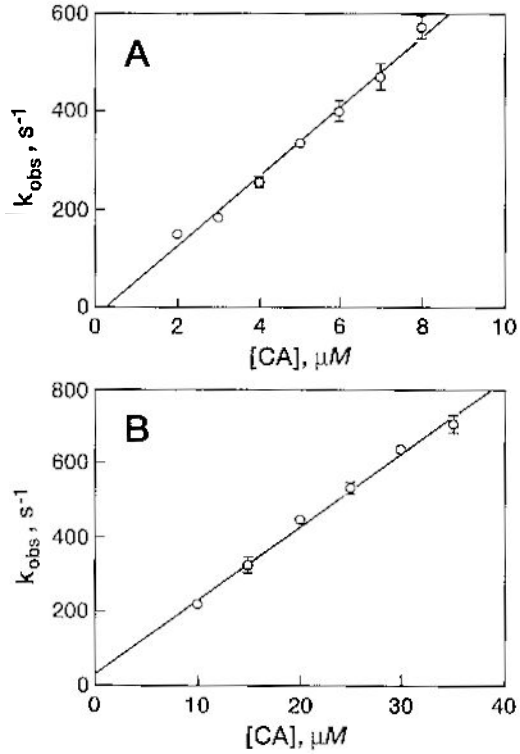

Figure 4. Plot of the pseudo-first-order rate constant, k_{obs}, *versus* [CA] for the reduction by CA of (A) HRP-I to HRP-II and (B) HRP-II to HRP. The slopes, k_{12} and k_{13} are (6.8 ± 0.2) × 10^7 M^{-1} s^{-1} and (2.1 ± 0.1) × 10^7 M^{-1} s^{-1}, respectively.

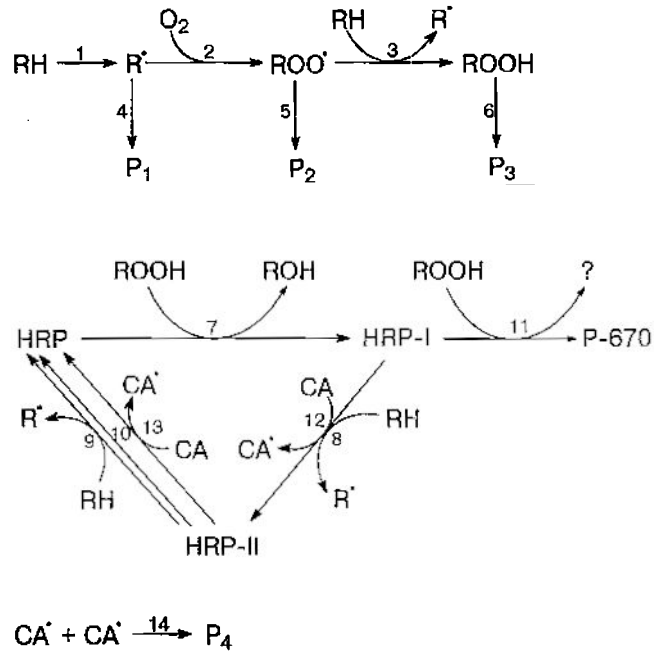

Figure 5. The model of peroxidase-catalyzed IAA oxidation in the presence of CA at neutral pH.

tion even before HRP addition, is enough to oxidize the entire amount of added CA. Therefore when [CA] < $[CA]_{cr}$ there is only a short delay of IAA oxidation. However, if [CA] > $[CA]_{cr}$ then the trace of ROOH in the IAA solution is consumed completely but CA is not completely oxidized. However, because ROOH continues to be produced slowly in the reaction mixture due to Reactions 1–3 then the remaining CA is slowly oxidized. Thus the delay caused by [CA] > $[CA]_{cr}$ is much longer than that caused by [CA] < $[CA]_{cr}$. The $[CA]_{cr}$ can be roughly estimated as 2 ×

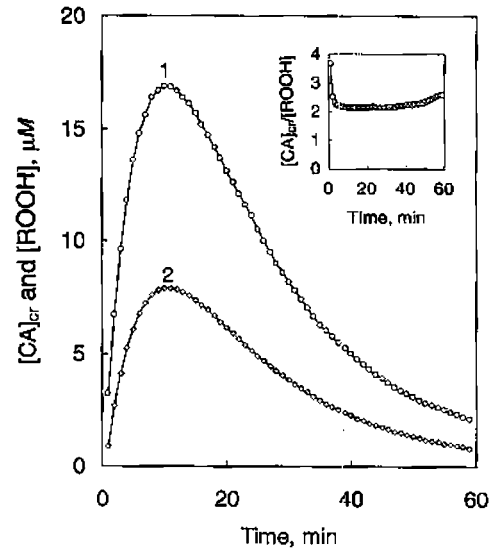

Figure 6. Computer simulation data $[CA]_{cr}$ as a function of time period between HRP and CA additions to IAA (curve 1) and [ROOH] at the time of CA addition (curve 2). Inset shows the ratio $[CA]_{cr}$/[ROOH].

$[ROOH]_0$ because one molecule of ROOH is required to oxidize two molecules of CA in the standard peroxidase cycle. The $[CA]_{cr}$ obtained from computer simulation is about 2.6 $\times$ $[ROOH]_0$. The simulated value is higher than the estimate of 2 $\times$ $[ROOH]_0$ because the estimate was obtained without taking into account that IAA oxidation starts when CA is not yet completely oxidized. Nakajima and Yamazaki estimated the ratio $[ascorbate]_{cr}/[ROOH]_0$ to be 1 (9). The discrepancy between the factors of 2, estimated by us, and 1, estimated by Nakajima and Yamazaki, could be due to either large experimental error in Yamazaki's measurements or an ability of ascorbate to act as a two-electron reductant, as does *p*-cresol (29). In our experiment on reduction of HRP-I by an equimolar amount of ascorbate, an equimolar amount of HRP-II was formed. Thus ascorbate is a one-electron reducing agent. Therefore we conclude that $[ascorbate]_{cr}$ was underestimated in Yamazaki's experiments.

We have developed a detailed model in the present study that can be used to explain earlier experimental results concerning the inhibition of IAA oxidation. It was reported that the inhibited reaction can be reinitiated by addition of second portion of IAA (9,14). In terms of our model a second addition of IAA is *per se* the addition of extra ROOH required for the oxidation of inhibitor. Therefore, a second portion of IAA can initiate the inhibited reaction.

The lag period caused by $[CA] > [CA]_{cr}$ decreases with increasing [HRP] up to a point where it becomes constant (15). According to our model Reactions 6 and 7 compete for ROOH, whereas Reaction 1 is the rate-limiting step in the chain reaction forming ROOH (Reactions 1–3). Reaction 7 is responsible for the initiation of the peroxidase cycle and subsequent oxidation of CA. The rate of Reaction 7 increases with increasing [HRP], whereas that of Reaction 6 does not depend on [HRP]. Therefore, the lag period decreases with increasing [HRP] until Reaction 1 limits the rate of Reaction 7 and a further decrease of the lag period is not observed.

Addition of CA after the reaction is started

If CA is added to IAA after the addition of enzyme then $[CA]_{cr}$ depends on the period of time from HRP addition to CA addition (Fig. 6). The spontaneous oxidation of IAA is started by HRP and the length of time it is allowed to proceed influences the effect of added inhibitor. The ratio $[CA]_{cr}/[ROOH]$ is close to 2 for almost the entire reaction time (Fig. 6, inset), so that $[CA]_{cr}$ depends mainly on [ROOH]. However, at the beginning and at the end of the reaction the ratio is higher.

The reaction mixture contains other intermediates that are able to initiate the oxidation of CA: ROO$^\cdot$, HRP-I and HRP-II. Previously we demonstrated that ROO$^\cdot$, HRP-I and HRP-II reach their steady-state concentrations in 1 min, whereas ROOH requires 10 min after reaction initiation (11). Therefore at the very beginning of IAA oxidation the ratio

$$\frac{[ROO^\cdot] + [HRP\text{-}I] + [HRP\text{-}II]}{[ROOH]}$$

is higher than in the steady state. We also demonstrated that HRP-I increases at the end of the reaction, whereas the concentrations of all other intermediates decrease (11). Therefore the above ratio is also higher at the end of the reaction. Each molecule of ROO$^\cdot$, ROOH and/or HRP-I is able to initiate oxidation of two molecules of CA (29), whereas HRP-II is able to oxidize only one molecule of CA. Therefore the following ratio is expected to be equal to unity:

$$\frac{[CA]_{cr}}{2 \times ([ROO^\cdot] + [ROOH] + [HRP\text{-}I]) + [HRP\text{-}II]}$$

The reasons for a ratio of one are the following. After addition of $[CA] \geq [CA]_{cr}$, IAA oxidation stops and R$^\cdot$, ROO$^\cdot$ and ROOH are no longer produced. All of the R$^\cdot$, ROO$^\cdot$, ROOH, HRP-I and HRP-II present at the time of addition of CA is consumed by CA oxidation. If $[CA] < [CA]_{cr}$ then CA is completely oxidized before the oxidizing species are consumed. The [R$^\cdot$] is not included in the above ratio because its concentration is far too small (11); and IAA does not compete with CA because k_{12} and $k_{13} \gg k_8$ and k_9. Using simulated kinetics of ROO$^\cdot$ ROOH, HRP-I and HRP-II as well as the $[CA]_{cr}$ determined in the computer analysis (Fig. 6), an average ratio of 0.999 $\pm$ 0.015 was calculated. This confirms that $[CA]_{cr}$ is equal to the sum of the concentrations of reaction intermediates able to initiate CA oxidation, multiplied by the number of molecules of CA, which they can oxidize. If the very beginning and the end of the reaction is excluded, the ratio $[CA]_{cr}/(2 \times [ROOH])$ is equal to 1.1 $\pm$ 0.2. Therefore the measurement of $[CA]_{cr}$ can be used for the experimental determination of [ROOH] in the reaction mixture with sufficiently high precision.

Chemiluminescence

It is known that the peroxidase-catalyzed oxidation of IAA produces chemiluminescence (6–8). The chemiluminescence consists of at least three spectral bands, the relative intensities of which depend upon experimental conditions. Therefore at least three emitting products are formed during the oxidation. However, only one of them, emitting at 420 nm, is predominant at neutral pH (6). The chemiluminescence produced by peroxidase-catalyzed IAA oxidation at neutral pH was proposed to be induced by hydroperoxide molecules, ROOH (8). Our present paper establishes that the change in concentration of ROOH during IAA oxidation can be obtained by measurement of critical inhibitor concentration. Such kinetic data can be used to examine the hypothesis regarding the key role of ROOH in the chemiluminescence of the IAA/HRP/O_2 system at neutral pH.

Excluded reaction

We did not include the potentially important reaction (16,17)

$$R^\cdot + CA \xrightarrow{k_{15}} P_4 + CA^\cdot \qquad (15)$$

in the mechanism of inhibition (Fig. 5) because: (1) the contribution of Reaction 15 in consumption of R$^\cdot$ is much less than that of Reaction 2, and (2) the contribution of Reaction 15 in the reaction of CA is much less than that of Reactions 12 and 13. The disappearance of R$^\cdot$ can be compared for Reactions 2 and 15 using the following values: $k_2 = 10^8\ M^{-1}\ s^{-1}$ (30), $[O_2] = 2.5 \times 10^{-4}\ M$ (26), $k_{15} \leq 10^9\ M^{-1}\ s^{-1}$ (diffusion-controlled limit), $[CA] = 10^{-7}\ M$ (typical concentration in the present study). Furthermore, $k_2\ [O_2] = 2.5 \times 10^4$

s^{-1} and k_{15} [CA] $\leq 10^2$ s^{-1}. That is, k_2 [O_2] $\gg k_{15}$ [CA]. Thus the contribution of Reaction 2 in R' uptake is much more than that of Reaction 15. The uptake of CA is not so obvious because Reactions 12 and 13 are preceded by Reactions 2, 3 and 7. We used computer simulation to compare the uptake of CA in Reaction 15 to that in Reactions 12 and 13. We assumed a diffusion-controlled-limit value for k_{15} of 10^9 M^{-1} s^{-1} and calculated the contributions of enzymatic (Reactions 12 and 13) and nonenzymatic (Reaction 15) pathways to the uptake of CA. We found that the nonenzymatic pathway competed with the enzymatic one only when [CA] $> 10^{-5}$ M, which is much greater than the [CA] used in the present study. Therefore, Reaction 15 is not included in the mechanism of inhibition and we concluded that CA inhibits IAA oxidation as a competitive substrate, not as a free radical scavenger.

Limitations

The model we have developed describes most of the experimental data quantitatively. However there are some limitations. The time curves of change in [HRP-II] during the peroxidase-catalyzed IAA oxidation in the presence of CA show that the shape of the kinetic traces depend on [CA] (Fig. 1B). For [CA] > $[CA]_{cr}$ the maxima in [HRP-II] are reached in 1–2 min after reaction initiation, whereas if [CA] > $[CA]_{cr}$ the maxima in [HRP-II] are reached 15–30 min after reaction reinitiation. Our model does not describe the effect of CA on the shape of HRP-II kinetic traces. Simulated kinetics of HRP-II does not depend on [CA] except for the delay period. The effect of CA on HRP-II formation needs more experimental investigation. The shapes of the kinetic traces of IAA oxidation are not affected by CA in contrast to those for HRP-II (Fig. 1A). They are similar within experimental error and the delay of the initiation of the reaction is the only difference between them. This is in agreement with the results of Nakajima and Yamazaki (9).

Acknowledgement—This research was supported by the Natural Sciences and Engineering Research Council of Canada.

REFERENCES

1. Dorffling, K. (1982) *Das Hormonsystem der Pflanzen.* Georg Tieme Verlag, Stuttgart.
2. Cilento, G. (1980) Photobiochemistry in the dark. *Photochem. Photobiol. Rev.* **5**, 109–228.
3. Cilento, G. (1984) Generation of electronically excited triplet species in biochemical systems. *Pure Appl. Chem.* **56**, 1179–1190.
4. Cilento, G. and W. Adam (1988) Photochemistry and photobiology without light. *Photochem. Photobiol.* **48**, 109–228.
5. Cilento, G. (1988) Photobiochemistry without light. *Experientia* **44**, 572–576.
6. Krylov, S. N., V. V. Lazarev and L. B. Rubin (1990) Kinetics associated with chemiluminescence spectra during oxidation of heteroauxin by peroxidase. *Dokl. Biophys.* **310**, 28–31.
7. Escobar, J. A., J. Vasquez-Vivar and G. Cilento (1992) Free radicals and excited species in the metabolism of indole-3-acetic acid and its ethyl ester by horseradish peroxidase and by neutrophils. *Photochem. Photobiol.* **55**, 895–902.
8. De Melo, M. P., J. A. Escobar, D. Metodiewa, H. B. Dunford and G. Cilento (1992) Horseradish peroxidase-catalyzed aerobic oxidation of indole-3-acetic acid. II. Oxygen uptake and chemiluminescence. *Arch. Biochem. Biophys.* **296**, 34–39.
9. Nakajima, R. and I. Yamazaki (1979) The mechanism of indole-3-acetic acid oxidation by horseradish peroxidase. *J. Biol. Chem.* **254**, 872–878.
10. Krylov, S. N. and H. B. Dunford (1995) Evidence for a free radical chain mechanism in the reaction between peroxidase and indole-3-acetic acid at neutral pH. *Biophys. Chem.* (In press)
11. Krylov, S. N. and H. B. Dunford (1996) Detailed model of the peroxidase-catalyzed oxidation of indole-3-acetic acid at neutral pH. *J. Phys. Chem.* **100**, 913–920.
12. Krylov, S. N. and A. B. Chebotareva (1993) Peroxidase-catalyzed co-oxidation of indole-3-acetic acid and xanthene dyes in the absence of hydrogen peroxide. *FEBS Lett.* **324**, 6–8.
13. Wu, T. W., L. H. Zeng, J. Wu and K. P. Fung (1993) Morin hydrate is a plant-derived and antioxidant-based hepatoprotector. *Life Sci.* **53**, PL213–218.
14. Krylov, S. N., S. M. Krylova and L. B. Rubin (1993) Threshold effect of caffeic acid on peroxidase-catalyzed oxidation of indole-3-acetic acid. *Phytochemistry* **33**, 9–12.
15. Krylov, S. N., S. M. Krylova, I. G. Chebotarev and A. B. Chebotareva (1994) Inhibition of enzymatic indole-3-acetic acid oxidation by phenols. *Phytochemistry* **36**, 263–267.
16. Krylov, S. N., B. D. Aguda and M. L. Ljubimova (1995) Bistability and reaction thresholds in the phenol-inhibited peroxidase-catalyzed oxidation of indole-3-acetic acid. *Biophys. Chem.* **53**, 213–218.
17. Sacher, J. A. (1962) An IAA oxidase–inhibitor system in bean pods. II. Kinetic studies of oxidase and natural inhibitor. *Plant Physiol.* **37**, 74–82.
18. Sacher, J. A. (1963) Effect of inhibitors on kinetics of indole-acetic acid oxidation. *Am. J. Bot.* **50**, 116–122.
19. Schaeffer, G. W., J. G. Buta and F. Sharpe (1967) Scopoletin and polyphenol-induced lag in peroxidase catalyzed oxidation of indole-3-acetic acid. *Physiol. Plant.* **20**, 342–347.
20. Stonier, T., Y. Yoneda and F. Rodriguez-Tormes (1968) Studies on auxin protectors. V. On the mechanism of IAA protection by protector-I of the Japanese morning glory. *Plant Physiol.* **43**, 1141–1145.
21. Gelinas, D. A. (1973) Proposed model for the peroxidase-catalyzed oxidation of indole-3-acetic acid in the presence of the inhibitor ferulic acid. *Plant Physiol.* **51**, 967–972.
22. Lee, T. T. (1977) Role of phenolic inhibitors in peroxidase-mediated degradation of indole-3-acetic acid. *Plant Physiol.* **59**, 372–375.
23. Lee. T. T., G. L. Rock and A. Stoessl (1978) Effect of orchinol and related phenanthrenes on the enzymic degradation of indole 3-acetic acid. *Phytochemistry* **17**, 1721–1726.
24. Grambow, H. J. and B. Langenbeck-Schwich (1983) The relationship between oxidase activity, peroxidase activity, hydrogen peroxide, and phenolic compounds in the degradation of indole-3-acetic acid *in vitro*. *Planta* **157**, 131–137.
25. Ohlsson, P.-I. and K.-G. Paul (1976) The molar absorptivity of horseradish peroxidase. *Acta Chem. Scand.* **B30**, 373–375.
26. Robinson, J. and J. M. Cooper (1970) Method of determining oxygen concentration in biological media, suitable for calibration of the oxygen electrode. *Anal. Biochem.* **33**, 390–399.
27. Press, W. H., B. P. Flannery, S. A. Tenkolsky, and W. T. Vetterling (1992) *Numerical Recipes. The Art of Scientific Computing.* Cambridge University Press, Cambridge.
28. Yamazaki, H. and I. Yamazaki (1973) The reaction between indole-3 acetic acid and horseradish peroxidase. *Arch. Biochem. Biophys.* **154**, 147–159.
29. Hewson, W. D. and H. B. Dunford (1976) Stoichiometry of the reaction between horseradish peroxidase and *p*-cresol. *J. Biol. Chem.* **251**, 6043–6052.
30. Candeias, L. P., L. K. Folkes, M. F. Dennis, K. B. Patel, S. A. Everett, M. R. L. Stratford and P. Wardman (1994) Free radical intermediates and stable products in the oxidation of indole-3-acetic acid. *J. Phys. Chem.* **98**, 10131–10137.